

Investigation of Enhanced Inertial Navigation Algorithms by Functional Iteration

Abstract—The defects of the traditional strapdown inertial navigation algorithms become well acknowledged and the enhanced traditional algorithms have been quite recently proposed trying to mitigate both theoretical and algorithmic defects. In this paper, the analytical accuracy evaluation of both the traditional algorithms and the enhanced algorithms is investigated, against the true reference for the first time enabled by the functional iteration approach having provable convergence. The analyses by the help of MATLAB Symbolic Toolbox show that the resultant error orders of all algorithms under investigation are consistent with those in the existing literatures, and yet the effect of the enhanced algorithms is marginal. Numerical results agree with analyses that the enhanced algorithms have marginal accuracy improvement over the traditional algorithms, while the functional iteration approach possesses significant accuracy superiority even in sustained lowly dynamic conditions.

Index Terms—Enhanced algorithms, functional iteration approach, accuracy evaluation, lowly dynamic conditions.

I. INTRODUCTION

Attitude, velocity, and position information are essential to many fields, such as aerospace, driverless vehicles, robotics, and computer vision. The inertial navigation system acquires these information by integrating inertial measurements from gyroscopes and accelerometers [1, 2].

The traditional inertial navigation algorithm is based on a two-speed structure, and focuses on the coning/sculling/scrolling corrections when integrating attitude/velocity/position differential equations [3], wherein the coning and sculling corrections are the dominating factors of algorithm accuracy in dynamic

This work was supported in part by National Natural Science Foundation of China (62273228) and Shanghai Jiao Tong University Scientific and Technological Innovation Funds (*Corresponding author: Yuanxin Wu*).

Authors' address: Hongyan Jiang, Maoran Zhu, and Yuanxin Wu are with the Shanghai Key Laboratory of Navigation and Location-based Services, School of Electronic Information and Electrical Engineering, Shanghai Jiao Tong University, Shanghai 200240, China, E-mail: (hy_jiang@sjtu.edu.cn; zhumaoran@sjtu.edu.cn; yuanx_wu@hotmail.com).

motions [4]. In more than half a century, a great number of researches have been devoted to attitude and velocity computation [4, 5]. Goodman and Robinson [6] proposed the simplified rotation vector differential equation of three-axis angular motions to obtain attitude by numerical integration. Savage [7] attempted to directly solve the direction cosine matrix (DCM) rate equation by the technique of two-order Picard iteration. Jordan [8] proposed the two-speed structure algorithm based on the rotation vector-DCM/quaternion combined representation, wherein the high-speed computation part was founded on the simplified Goodman-Robinson rotation vector differential equation, the low-speed computation part took the rotation vector from the high-speed computation part as the input, and the DCM/quaternion representation was used for global attitude update. In the light of the earlier work by Laning [9] in 1949, Bortz [10] proposed the exact rotation vector differential equation, which, together with Jordan's two-speed structure, established the foundation of the traditional inertial navigation algorithm [11]. Miller [12] proposed that the classical coning motion should be considered as the design base for optimizing the coning correction. For the traditional velocity computation, the first-order approximation of attitude matrix has been generally adopted in the transformed specific force integration [3, 13], while a second-order approximation was highlighted by Ignagni in [2]. It is based on the exact velocity rotation compensation proposed by Savage in [13] but has not been widely exploited so far in the community.

In fact, the traditional inertial navigation algorithms possess major defects in both theory and algorithm aspects [14]. In the theory aspect, the approximate second-order integration of the rotation vector is widely used for attitude computation, and the first-order approximation of attitude matrix is commonly adopted in velocity computation. Besides, the traditional inertial navigation algorithm is usually designed under such special motion forms as the classical coning/sculling motions. Ignagni [15] noted that the influence of rotation vector approximation on a high-precision inertial navigation system could be ignored. However, Musoff [16] reported that using the classical coning motion as the algorithm design base was suboptimal under other motion forms. Notably, the collaborative work [17] revealed the importance of the neglected high-order terms of rotation vector rate equation. Savage [11] proposed a unified framework of attitude/velocity/position computation by extending the concept of rotation vector to velocity/position translation vectors. Yan [18] identified a significant problem of the error evaluation in the coning correction algorithm design, namely, the attitude accuracy cannot

be improved unlimitedly by increasing the number of gyroscope samples in the traditional attitude algorithm. In the light of Taylor series expansion, Song [19] analyzed the errors of the velocity integration algorithm with the exact rotation compensation term (ViaErc) in [13] and the general velocity integration algorithm based on the simplified rotation and velocity translation vectors (ViaGen) in [11], which were both raised by Savage. In addition, Wu [20, 21] proposed the velocity/position integration formulae to rigorously tackle the navigation frame rotation issue in the traditional velocity/position computation.

The functional iteration algorithms [14, 22-24] were recently raised to directly solve the exact inertial navigation differential equations, achieving state-of-the-art ultra-high precision navigation computation. Specifically, Wu [22] introduced the functional iteration method to accurately solve the Rodrigues vector differential equation in view of its simpler form than that of the rotation vector. A faster version was further proposed in [23] by transforming the Rodrigues vector polynomial iteration into the Chebyshev polynomial coefficients iteration, where the technique of polynomial truncation was used to alleviate the computing burden without impairing the accuracy. Wu [14] further applied the functional iteration method and Chebyshev polynomial approximation to achieve the whole inertial navigation computation (iNavFIter) and reduced the noncommutativity errors to almost machine precision. Besides, under the eight-sample scenario, Wu and Litmanovich [25] numerically compared the attitude accuracies of the Taylor series expansion and functional iteration method. Quite recently, Ignagni [4, 5] stressed the significant shortcomings of the traditional algorithms under sustained highly dynamic motions, and consequently proposed the enhanced algorithms for better accuracy.

This paper aims to analytically investigate the accuracy of the traditional algorithms and the enhanced algorithms against the functional iteration algorithm (details referred to [14]), focusing on the accuracy improvement effect of the enhanced algorithms. The main contribution of the current work is that the functional iteration approach, by the aid of MATLAB Symbolic Toolbox, is proposed to serve as a convenient accuracy evaluation benchmark, and the analytical accuracy evaluation of the traditional/enhanced algorithms has been performed for the first time against the functional iteration approach, throwing light on marginal accuracy gains of the enhanced algorithms over the traditional algorithms. Moreover, the extra accuracy superiority of the functional iteration approach under sustained lowly dynamic conditions is newly highlighted by numerical results. The rest of the paper

is structured as follows. Section II briefly summarizes the traditional and enhanced algorithms. Algorithms of interest are analyzed in the two-sample case as a demo for the sake of balance between theoretical rigor and presentation brevity. In Section III, the error orders of the traditional/enhanced algorithms, the ViaGen algorithm, and the functional iteration algorithm are analyzed and verified with the help of MATLAB Symbolic Toolbox. In Section V, in both the two-sample and four-sample cases, all algorithms are numerically compared under the customarily-designed trajectory. Conclusions are drawn in Section VI.

II. TRADITIONAL INERTIAL NAVIGATION ALGORITHMS

Suppose the computation time interval is $[0, T]$ with any time t satisfying $0 \leq t \leq T$ and T denotes the time interval length. At time instants t_k ($k = 1, 2, \dots$) within the computation time interval, assuming the discrete measurements outputted by gyroscopes and accelerometers are given, the goal is to obtain the attitude, velocity, and position. The body frame is denoted by the symbol b , and the navigation frame is denoted by the symbol n . The navigation frame in this paper adopts the definition of North-Up-East [21] without loss of generality.

A. Attitude Computation

According to the chain rule of the attitude matrix, \mathbf{C}_b^n at any time satisfies

$$\mathbf{C}_b^n(t) = \mathbf{C}_{b(t)}^{n(t)} = \mathbf{C}_{n(0)}^{n(t)} \mathbf{C}_{b(0)}^{b(0)} \mathbf{C}_{b(t)}^{b(0)} = \mathbf{C}_{n(0)}^{n(t)} \mathbf{C}_b^n(0) \mathbf{C}_{b(t)}^{b(0)} \quad (1)$$

where $\mathbf{C}_{b(0)}^{b(t)}$ and $\mathbf{C}_{n(0)}^{n(t)}$ describe the attitude changes of the body frame and the navigation frame from time 0 to t , respectively. The quaternion parameterization is chosen in this paper, namely, $\mathbf{q} = [s \ \mathbf{\eta}^T]^T$, where s is the scalar part and $\mathbf{\eta}$ is the vector part. The rotation vector is represented by $\boldsymbol{\sigma} = \sigma \mathbf{e}$, where \mathbf{e} denotes the unit vector of a fixed axis and σ denotes the magnitude of the rotation, and then, the quaternion can be expressed by a nonzero rotation vector as follows [1]

$$\mathbf{q} = \cos \frac{\sigma}{2} + \frac{\boldsymbol{\sigma}}{\sigma} \sin \frac{\sigma}{2} \quad (2)$$

In view of (1), the attitude computation can be divided into two independent parts [2, 26], $\mathbf{q}_{b(0)}^{b(t)}$ and $\mathbf{q}_{n(0)}^{n(t)}$, both of which have the same function form with respect to rotation vector as (2), with the former related to $\boldsymbol{\sigma}_b$ and

the latter related to $\boldsymbol{\sigma}_n$. Notably, $\boldsymbol{\sigma}_b$ is the rotation vector in the body frame, satisfying [10]

$$\dot{\boldsymbol{\sigma}}_b = \boldsymbol{\omega}^b + \frac{1}{2} \boldsymbol{\sigma}_b \times \boldsymbol{\omega}^b + \frac{1}{\sigma_b^2} \left[1 - \frac{\sigma_b \sin \sigma_b}{2(1 - \cos \sigma_b)} \right] \boldsymbol{\sigma}_b \times (\boldsymbol{\sigma}_b \times \boldsymbol{\omega}^b) \quad (3)$$

where the subscript of $\boldsymbol{\omega}_{ib}^b$ is omitted for symbolic brevity. Besides, $\boldsymbol{\sigma}_n$ denotes the rotation vector in the navigation frame and satisfies the same differential equation form as in (3). However, the rotation vector in the navigation frame is usually approximated by $\boldsymbol{\sigma}_n = T \boldsymbol{\omega}_m^n$ since the navigation frame rotates rather slowly [2].

The main aim of the traditional attitude algorithm is to solve (3) for $\boldsymbol{\sigma}_b$. In practice, a simplified form of (3), also known as the simplified Goodman-Robinson rotation vector differential equation, is generally given as follows [6, 8, 27, 28]

$$\dot{\boldsymbol{\sigma}}_b = \boldsymbol{\omega}^b + \frac{1}{2} \mathbf{a} \times \boldsymbol{\omega}^b \quad (4)$$

where the angular increment is defined as $\mathbf{a} = \int_0^t \boldsymbol{\omega}^b dt$.

Suppose the angular velocity is expressed as a polynomial of time as $\boldsymbol{\omega}^b = \mathbf{a}_\omega + \mathbf{b}_\omega t$, where \mathbf{a}_ω and \mathbf{b}_ω are constant vector coefficients. Note that the above linear form is used just for a balance between theoretical rigor and presentation brevity. Then the approximate rotation vector can be obtained by integrating (4) on the computation time interval, say

$$\tilde{\boldsymbol{\sigma}}_b \approx \mathbf{a}_\omega t + \mathbf{b}_\omega \frac{t^2}{2} + \mathbf{a}_\omega \times \mathbf{b}_\omega \frac{t^3}{12} \quad (5)$$

The above polynomial coefficients can be readily obtained using the angular increments measured by gyroscopes, see e.g. [20], and thus $\tilde{\boldsymbol{\sigma}}_b$ can be readily solved.

Ignagni [2, 5] analyzed the theoretical errors implicit in the simplified Goodman-Robinson rotation vector differential equation and proposed an enhanced attitude algorithm. Specifically, the approximate rotation vector $\tilde{\boldsymbol{\sigma}}_b$ is substituted into the right side of (3), and the scalar coefficient of the third term is approximated as 1/12, say

$$\dot{\boldsymbol{\sigma}}_b = \boldsymbol{\omega}^b + \frac{1}{2} \tilde{\boldsymbol{\sigma}}_b \times \boldsymbol{\omega}^b + \frac{1}{12} \tilde{\boldsymbol{\sigma}}_b \times (\tilde{\boldsymbol{\sigma}}_b \times \boldsymbol{\omega}^b) \quad (6)$$

Similarly, the refined rotation vector $\boldsymbol{\sigma}_b$ is obtained as $\boldsymbol{\sigma}_b \triangleq \tilde{\boldsymbol{\sigma}}_b + \delta \boldsymbol{\sigma}_b$, where the compensated rotation vector part, $\delta \boldsymbol{\sigma}_b$, is defined as follows

$$\begin{aligned}
& \delta\sigma_b \\
&= \left[(\mathbf{a}_\omega \times \mathbf{b}_\omega) \times \mathbf{b}_\omega + \frac{1}{3} \mathbf{a}_\omega \times ((\mathbf{a}_\omega \times \mathbf{b}_\omega) \times \mathbf{a}_\omega) \right] \frac{t^5}{240} \\
&+ \left[\mathbf{a}_\omega \times ((\mathbf{a}_\omega \times \mathbf{b}_\omega) \times \mathbf{b}_\omega) + \frac{1}{2} \mathbf{b}_\omega \times ((\mathbf{a}_\omega \times \mathbf{b}_\omega) \times \mathbf{a}_\omega) \right] \frac{t^6}{864} \\
&+ \left[\mathbf{b}_\omega \times ((\mathbf{a}_\omega \times \mathbf{b}_\omega) \times \mathbf{b}_\omega) + \frac{1}{6} (\mathbf{a}_\omega \times \mathbf{b}_\omega) \times ((\mathbf{a}_\omega \times \mathbf{b}_\omega) \times \mathbf{a}_\omega) \right] \frac{t^7}{2016} \\
&+ (\mathbf{a}_\omega \times \mathbf{b}_\omega) \times ((\mathbf{a}_\omega \times \mathbf{b}_\omega) \times \mathbf{b}_\omega) \frac{t^8}{13824} \tag{7}
\end{aligned}$$

It should be highlighted that the additional algorithmic attitude error, as defined in [5] as the errors in integrating the simplified rotation-vector equation, depends on the specific optimized coning-compensation algorithm. For example, the algorithmic error vanishes in the two-sample case (the coefficient C is zero in Table II of [29]) but does not otherwise.

B. Velocity Computation

In terms of velocity computation in the traditional algorithm, the velocity update equation is shown as follows [2, 26]

$$\begin{aligned}
& \mathbf{v}^n \\
& \approx \mathbf{v}^n(0) + \mathbf{C}_{b(0)}^{n(0)} \int_0^t \mathbf{C}_{b(t)}^{b(0)} \mathbf{f}^b dt \\
& - \int_0^t (2\omega_{ie}^n + \omega_{en}^n) \times \mathbf{v}^n dt + \int_0^t \mathbf{g}^n dt + \Delta\mathbf{v}_f^c \\
& = \mathbf{v}^n(0) + \mathbf{C}_{b(0)}^{n(0)} \int_0^t \left[\mathbf{I} + \frac{\sin \sigma_b}{\sigma_b} (\sigma_b \times) + \frac{1 - \cos \sigma_b}{\sigma_b^2} (\sigma_b \times)^2 \right] \mathbf{f}^b dt \\
& - \int_0^t (2\omega_{ie}^n + \omega_{en}^n) \times \mathbf{v}^n dt + \int_0^t \mathbf{g}^n dt + \Delta\mathbf{v}_f^c \tag{8}
\end{aligned}$$

where the integration of the transformed specific force is denoted as $\mathbf{C}_{b(0)}^{n(0)} \int_0^t \mathbf{C}_{b(t)}^{b(0)} \mathbf{f}^b dt \triangleq \mathbf{u}$, and $\Delta\mathbf{v}_f^c$ is the compensation term due to the rotation of the navigation frame over the computational interval, defined by [2, 4, 13]

$$\Delta\mathbf{v}_f^c = -\frac{T}{2} (\omega_{ie}^n + \omega_{en}^n) \times (\mathbf{C}_{b(0)}^{n(0)} \mathbf{v}) \tag{9}$$

where the velocity increment $\mathbf{v} = \int_0^t \mathbf{f}^b dt$. Generally, the gravity vector and Coriolis acceleration change slowly during the usually short computing time interval, so the last two terms of (8) can be approximated as [2, 26]

$$\begin{aligned}
& \Delta\mathbf{v}_g \triangleq -\int_0^t (2\omega_{ie}^n + \omega_{en}^n) \times \mathbf{v}^n dt + \int_0^t \mathbf{g}^n dt \\
& \approx \left[\mathbf{g}^n - (2\omega_{ie}^n + \omega_{en}^n) \times \mathbf{v}^n \right] t \tag{10}
\end{aligned}$$

Typically, the simplified velocity update equation, up to the first-order angular increment, is given as [2, 3, 11, 13]

$$\mathbf{v}^n \approx \mathbf{v}^n(0) + \mathbf{C}_{b(0)}^{n(0)} \int_0^t (\mathbf{I} + (\mathbf{a} \times)) \mathbf{f}^b dt + \Delta\mathbf{v}_g + \Delta\mathbf{v}_f^c \tag{11}$$

where $\int_0^t \mathbf{a} \times \mathbf{f}^b dt$ is the commonly-used first-order velocity correction [2]. For the same brevity consideration, assume that the specific force is also represented as a linear polynomial of time, $\mathbf{f}^b = \mathbf{a}_f + \mathbf{b}_f t$, where \mathbf{a}_f and \mathbf{b}_f are constant vector coefficients. The integral term of (11) can be rewritten as [20]

$$\begin{aligned}
& \int_0^t (\mathbf{I} + (\mathbf{a} \times)) \mathbf{f}^b dt \\
& = \mathbf{v} + \frac{1}{2} (\mathbf{a}_\omega \times \mathbf{a}_f) t^2 + \frac{1}{3} \left(\frac{1}{2} \mathbf{b}_\omega \times \mathbf{a}_f + \mathbf{a}_\omega \times \mathbf{b}_f \right) t^3 \\
& + \frac{1}{8} (\mathbf{b}_\omega \times \mathbf{b}_f) t^4 \tag{12}
\end{aligned}$$

On the other hand, the simplified velocity update equation, up to the second-order angular increment, is given as [2, 4]

$$\begin{aligned}
& \mathbf{v}^n \approx \mathbf{v}^n(0) + \mathbf{C}_{b(0)}^{n(0)} \int_0^t \left[\mathbf{I} + (\mathbf{a} \times) + \frac{1}{2} (\mathbf{a} \times)^2 \right] \mathbf{f}^b dt \\
& + \Delta\mathbf{v}_g + \Delta\mathbf{v}_f^c \tag{13}
\end{aligned}$$

The term $\int_0^t \frac{1}{2} (\mathbf{a} \times)^2 \mathbf{f}^b dt$ is called the second-order velocity correction [2], where \mathbf{a}^b and \mathbf{f}^b are further approximately considered as constants. Thus the simplified second-order velocity correction is calculated as [2, 4]

$$\int_0^t \frac{1}{2} (\mathbf{a} \times)^2 \mathbf{f}^b dt \approx \frac{1}{6} \mathbf{a} \times (\mathbf{a} \times \mathbf{v}) \tag{14}$$

Therefore, the second-order velocity update equation is further approximated as follows [2, 4]

$$\begin{aligned}
& \mathbf{v}^n \approx \mathbf{v}^n(0) + \mathbf{C}_{b(0)}^{n(0)} \left[\int_0^t (\mathbf{I} + (\mathbf{a} \times)) \mathbf{f}^b dt + \frac{1}{6} \mathbf{a} \times (\mathbf{a} \times \mathbf{v}) \right] \\
& + \Delta\mathbf{v}_g + \Delta\mathbf{v}_f^c \tag{15}
\end{aligned}$$

In the case of two-sample algorithm, the term in the square bracket of (15) can be represented by constant vector coefficients \mathbf{a}_ω , \mathbf{b}_ω , \mathbf{a}_f and \mathbf{b}_f . The specific expression is not explicitly given here to avoid verbosity.

Hereafter, the algorithms based on the velocity update equation (11) and (15) are called the traditional first-order and traditional second-order algorithms, respectively. The latter shares the same spirit as the

ViaErc algorithm [13, 19]. It can be readily shown that the ViaErc algorithm is equivalent to the traditional second-order algorithm in (15).

It is obvious that both the first-order and second-order velocity corrections are undermined with potentially significant approximation errors, which were recently reiterated and compensated by an enhanced velocity algorithm in [2, 4]. The theoretical error in the first-order velocity correction is [2, 4]

$$\delta \mathbf{v}_1 = \int_0^t [\tilde{\mathbf{\sigma}}_b - \mathbf{a}] \times \mathbf{f}^b dt \quad (16)$$

and the theoretical error in the second-order velocity correction is [2, 4]

$$\delta \mathbf{v}_2 = \frac{1}{2} \int_0^t \tilde{\mathbf{\sigma}}_b \times [\tilde{\mathbf{\sigma}}_b \times \mathbf{f}^b] dt - \mathbf{a} \times (\mathbf{a} \times \mathbf{v}) / 6 \quad (17)$$

For the linear motion form, the theoretical errors implicit in the first-order and the second-order velocity corrections can be specifically derived as follows, respectively,

$$\delta \mathbf{v}_1 = (\mathbf{a}_\omega \times \mathbf{b}_\omega) \times \mathbf{a}_f \frac{t^4}{48} + (\mathbf{a}_\omega \times \mathbf{b}_\omega) \times \mathbf{b}_f \frac{t^5}{60} \quad (18)$$

$$\begin{aligned} \delta \mathbf{v}_2 = & \left[2\mathbf{a}_\omega \times (\mathbf{a}_\omega \times \mathbf{b}_f) - \mathbf{a}_\omega \times (\mathbf{b}_\omega \times \mathbf{a}_f) - \mathbf{b}_\omega \times (\mathbf{a}_\omega \times \mathbf{a}_f) \right] \frac{t^4}{48} \\ & + \left\{ \mathbf{a}_\omega \times (\mathbf{b}_\omega \times \mathbf{b}_f) + \mathbf{a}_\omega \times [(\mathbf{a}_\omega \times \mathbf{b}_\omega) \times \mathbf{a}_f] + \mathbf{b}_\omega \times (\mathbf{a}_\omega \times \mathbf{b}_f) \right. \\ & \left. - 2\mathbf{b}_\omega \times (\mathbf{b}_\omega \times \mathbf{a}_f) + (\mathbf{a}_\omega \times \mathbf{b}_\omega) \times (\mathbf{a}_\omega \times \mathbf{a}_f) \right\} \frac{t^5}{120} \\ & + \left\{ \mathbf{a}_\omega \times [(\mathbf{a}_\omega \times \mathbf{b}_\omega) \times \mathbf{b}_f] + \frac{1}{2} \mathbf{b}_\omega \times [(\mathbf{a}_\omega \times \mathbf{b}_\omega) \times \mathbf{a}_f] \right. \\ & \left. + (\mathbf{a}_\omega \times \mathbf{b}_\omega) \times (\mathbf{a}_\omega \times \mathbf{b}_f) + \frac{1}{2} (\mathbf{a}_\omega \times \mathbf{b}_\omega) \times (\mathbf{b}_\omega \times \mathbf{a}_f) \right\} \frac{t^6}{144} \\ & + \left\{ \mathbf{b}_\omega \times [(\mathbf{a}_\omega \times \mathbf{b}_\omega) \times \mathbf{b}_f] + (\mathbf{a}_\omega \times \mathbf{b}_\omega) \times (\mathbf{b}_\omega \times \mathbf{b}_f) \right. \\ & \left. + \frac{1}{6} (\mathbf{a}_\omega \times \mathbf{b}_\omega) \times [(\mathbf{a}_\omega \times \mathbf{b}_\omega) \times \mathbf{a}_f] \right\} \frac{t^7}{336} \\ & + (\mathbf{a}_\omega \times \mathbf{b}_\omega) \times [(\mathbf{a}_\omega \times \mathbf{b}_\omega) \times \mathbf{b}_f] \frac{t^8}{2304} \end{aligned} \quad (19)$$

Hence, the velocity update equations of the traditional first-order and second-order algorithms are respectively enhanced as follows [4, 5]

$$\mathbf{v}^n \approx \mathbf{v}^n(0) + \mathbf{C}_{b(0)}^{n(0)} \left[\int_0^t [\mathbf{I} + (\mathbf{a} \times)] \mathbf{f}^b dt + \delta \mathbf{v}_1 \right] + \Delta \mathbf{v}_g + \Delta \mathbf{v}_f^c \quad (20)$$

$$\begin{aligned} \mathbf{v}^n \approx & \mathbf{v}^n(0) + \mathbf{C}_{b(0)}^{n(0)} \left[\int_0^t [\mathbf{I} + (\mathbf{a} \times)] \mathbf{f}^b dt + \frac{1}{6} \mathbf{a} \times (\mathbf{a} \times \mathbf{v}) \right. \\ & \left. + \delta \mathbf{v}_1 + \delta \mathbf{v}_2 \right] + \Delta \mathbf{v}_g + \Delta \mathbf{v}_f^c \end{aligned} \quad (21)$$

Hereafter, (20) and (21) are called the enhanced first-order and second-order algorithms, respectively. Due to the page limit, the subsequent sections will focus on the second-order algorithm. By analogy, the algorithmic errors of the velocity algorithm was also defined in [4] that vanishes as well for the two-sample case (the coefficients \mathbf{d} and \mathbf{g} are zeros in Table III of [30]).

Furthermore, a brief review of the ViaGen algorithm is also given below for a comprehensive accuracy comparison. Specifically, the integration of the transformed specific force therein is [13, 19]

$$\begin{aligned} \mathbf{u}_{Gen} = & \mathbf{C}_{b(0)}^{n(0)} \left[\mathbf{\eta} + \frac{1 - \cos \tilde{\sigma}_b}{\tilde{\sigma}_b^2} \tilde{\mathbf{\sigma}}_b \times \mathbf{\eta} + \frac{1}{\tilde{\sigma}_b^2} \left(1 - \frac{\sin \tilde{\sigma}_b}{\tilde{\sigma}_b} \right) \tilde{\mathbf{\sigma}}_b \times (\tilde{\mathbf{\sigma}}_b \times \mathbf{\eta}) \right] \\ \approx & \mathbf{C}_{b(0)}^{n(0)} \left[\mathbf{\eta} + \frac{1}{2} \tilde{\mathbf{\sigma}}_b \times \mathbf{\eta} + \frac{1}{6} \tilde{\mathbf{\sigma}}_b \times (\tilde{\mathbf{\sigma}}_b \times \mathbf{\eta}) \right] \end{aligned} \quad (22)$$

where the velocity translation vector $\mathbf{\eta}$ is approximately given as [13, 19]

$$\mathbf{\eta} = \mathbf{v} + \frac{1}{2} \int_0^t (\mathbf{a} \times \mathbf{f}^b - \mathbf{\omega} \times \mathbf{v}) dt \quad (23)$$

As for the position update, a compensation scheme was given in [4], wherein the Simpson formula was used instead of the trapezoidal formula to compute the above integral of the velocity. Because the scheme is tightly related to the specific definition of update interval and it is nontrivial to formulate the theoretical error therein for general cases, we do not take a closer look into the compensation scheme of position update in this paper.

III. ALGORITHM ACCURACY ANALYSIS

In this section, we accomplish the algorithm accuracy analysis by the aid of MATLAB Symbolic Toolbox, in contrast to the traditional manual mathematical derivation. By so doing, it helps us to spare the tedious mathematical details and concentrate on the main idea. Note that no compensation algorithm for the theoretical error implicit in the traditional position update was discussed in [4], so this paper focuses on the attitude and velocity computation accuracy.

The functional iteration approach is capable of provably solving the exact attitude and velocity update equations [14, 22, 24] and consequently obtaining the analytical solution of the true rotation vector and the true

Table I
Polynomial Coefficients of Inertial Attitude Computation in a Test Example

	t	t^2	t^3	t^4	t^5	t^6	t^7	t^8
Typical	4	5/2	-1/3	0	0	0	0	0
Enhanced	4	5/2	-1/3	0	-697/360	-11/24	-251/336	-625/1536
FIterTrue ($l=1$)	4	5/2	0	0	0	0	0	0
FIterTrue ($l=2$)	4	5/2	-1/3	119/96	71/40	3451/8640	1559/1120	264763/13824
FIterTrue ($l=3$)	4	5/2	-1/3	0	-1481/720	153/1280	88181/4032	51048661/1161216
FIterTrue ($l=4$)	4	5/2	-1/3	0	-697/360	-1535/2304	-213839/6048	-56149561/774144
FIterTrue ($l=5$)	4	5/2	-1/3	0	-697/360	-11/30	-39065/24192	-13712053/387072
FIterTrue ($l=6$)	4	5/2	-1/3	0	-697/360	-11/30	-3533/216	-8644241/258048
FIterTrue ($l=7,8$)	4	5/2	-1/3	0	-697/360	-11/30	-3533/216	-13663/4032

Note: ‘Typical’ denotes the traditional attitude algorithm, ‘Enhanced’ denotes the enhanced attitude algorithm, ‘FIterTrue’ denotes the functional iteration attitude algorithm that is used as the reference, and l denotes the functional iteration times.

Table II
Polynomial Coefficients of Essential Velocity Computation of \mathbf{u} in a Test Example

	t	t^2	t^3	t^4	t^5	t^6	t^7	t^8
Typical	4	3	19/3	167/12	-263/24	-403/24	0	0
Enhanced	4	3	19/3	149/24	-253/15	-6601/288	-935/168	-9797/2304
ViaGen-1	4	3	19/3	149/24	-1685/144	-1517/96	241/216	-785/216
ViaGen-8	4	3	19/3	59/6	-1541/144	-41113/1440	-129137/60480	0
FIterTrue	4	3	19/3	59/6	-212/15	-4987/180	7681/630	24079/360

Note: ‘Typical’ denotes the traditional second-order velocity algorithm, ‘Enhanced’ denotes the enhanced second-order velocity algorithm, ‘ViaGen-1’ denotes the ViaGen velocity algorithm with first-order series of trigonometric coefficients, ‘ViaGen-8’ denotes the ViaGen velocity algorithm with eight-order series of trigonometric coefficients, and ‘FIterTrue’ denotes the functional iteration velocity algorithm that is used as the reference.

velocity. In this regard, the error orders of the traditional/enhanced algorithms and the ViaGen algorithm can be analyzed against the functional iteration algorithm with the help of MATLAB Symbolic Toolbox, aiming to study the potential accuracy advantages of the enhanced algorithm and the ViaGen algorithm over the traditional algorithm. It should be noted that, when the functional iteration method is used to solve (3), the trigonometric function coefficient in the third term is expanded to the eighth-order Taylor series [25].

In the MATLAB symbolic development, the coefficients \mathbf{a}_ω , \mathbf{b}_ω , \mathbf{a}_f and \mathbf{b}_f are all generated as random integer vectors to make sure the derived conclusion has a general sense. However, in the sequel we just exemplify a specific set of vector coefficients for

concise demonstration. It should be highlighted that the following observations are consistent throughout all of our random vector coefficients results. Specifically, we set $\mathbf{a}_\omega = [4 \ 2 \ 3]^T$, $\mathbf{b}_\omega = [5 \ 8 \ 10]^T$, $\mathbf{a}_f = [4 \ 5 \ 6]^T$, and $\mathbf{b}_f = [9 \ 8 \ 7]^T$. The resultant polynomial coefficients of essential attitude and velocity computation are listed in Tables I and II, respectively. The attitude coefficient convergence process of the functional iteration algorithm across eight iterations is also shown in Table I.

With the result of the functional iteration algorithm as the reference, Table I shows that the error order of the traditional attitude algorithm is $O(t^5)$, consistent with the result in [5], and that of the enhanced attitude

algorithm is $O(t^6)$. Moreover, Table II shows that the error orders of the traditional/enhanced second-order velocity algorithms are both $O(t^4)$. This fact implies that the enhanced attitude and velocity algorithms might just have marginal accuracy improvement over the traditional counterparts. When the eight-order Taylor series of trigonometric coefficients in (22) is used, Table II indicates that the error order of the ViaGen algorithm is $O(t^5)$, agreeing with the analysis in [19]. However, when utilizing the first-order simplification of trigonometric coefficients, the ViaGen algorithm exhibits a decreased accuracy by one order of time. Moreover, the ViaGen algorithm with an eight-order series of trigonometric coefficients demonstrates one order of time higher accuracy than the second-order

algorithms, highlighting the positive impact of the new concept of velocity translation vector on accuracy improvement.

Note that the above-obtained conclusion is not limited to the first-order polynomial functions of angular velocity/specific force with respect to time t and it remains valid for high-order polynomials according to our extra tests, e.g., the third-order polynomials.

IV. NUMERICAL RESULTS

In line with our previous works [14, 21, 25], the flight test simulation therein is used for numerical comparison, where data is generated in the navigation frame and the analytical truth is available for accuracy evaluation. The vehicle is initially located at zero longitude/latitude/height, and moves eastward with an

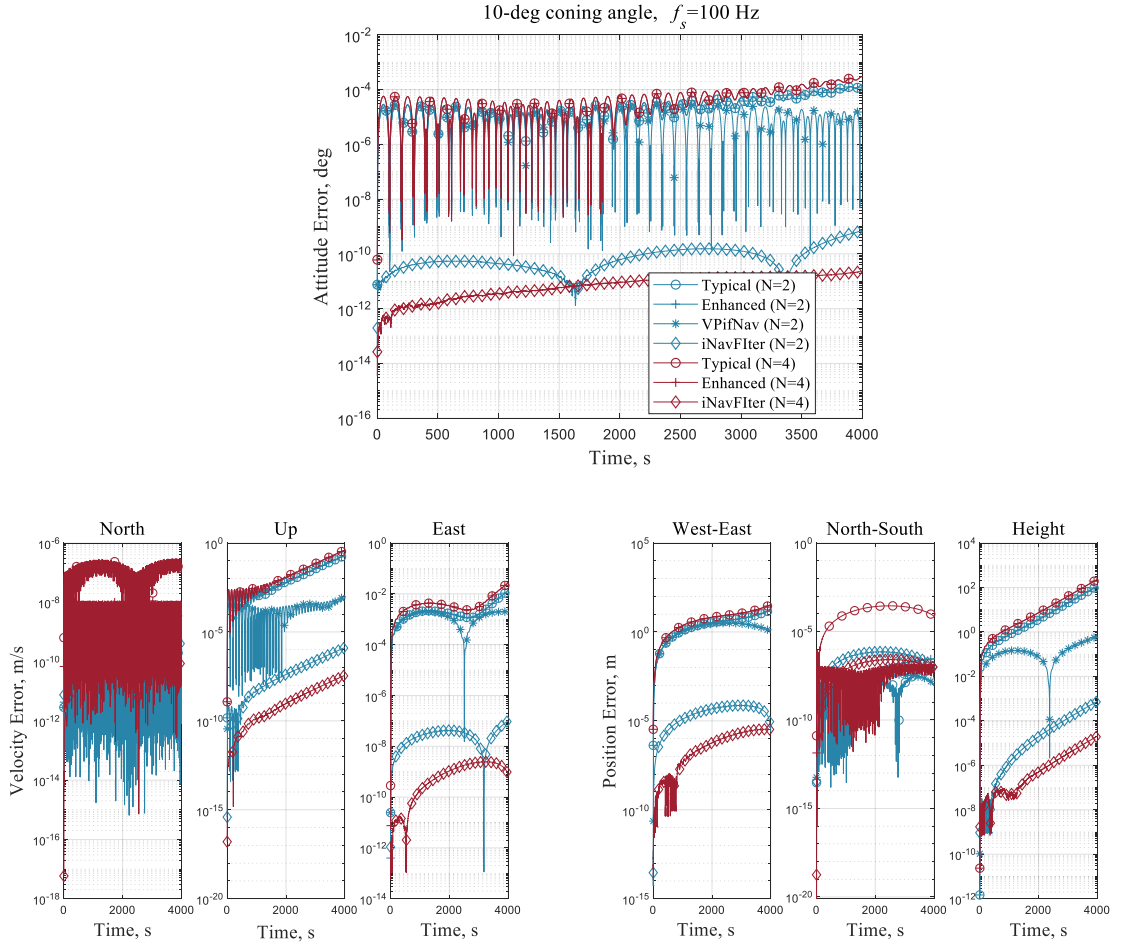


Fig. 1. Principal attitude error, velocity and position error of the typical/enhanced algorithms ($N=2, N=4$), the iNavFIter algorithm ($N=2, N=4$), and the VPifNav algorithm ($N=2$), for varying-speed coning flight.

initial speed $v_0 = 500 \text{ m/s}$ and velocity rate $\dot{\mathbf{v}}^n = [0 \ 0 \ a \sin(wt)]^T$, where a and w are the magnitude and angular frequency of the velocity rate ($a = 10 \text{ m/s}^2$, $w = 0.02 \text{ rad/s}$). Additionally, the body attitude undergoes a classical coning motion, which is described by attitude quaternion as [1]

$$\mathbf{q}_n^b = \cos(\zeta/2) + \sin(\zeta/2) [0 \cos(\Omega t) \sin(\Omega t)]^T \quad (24)$$

where ζ is the coning angle (unit: deg), $\Omega = 2\pi f_c$ is the angular frequency of the coning motion (unit: rad/s), and f_c is the coning frequency (unit: Hz). We set $\zeta = 10 \text{ deg}$ in this paper, and the sampling rate of gyroscopes and accelerometers is $f_s = 100 \text{ Hz}$.

For a fair peer comparison with [4, 5], the accuracy of all traditional/enhanced second-order algorithms is investigated in both the two-sample and the four-sample cases. In specific, both implicit and algorithmic errors of the traditional four-sample algorithm are taken into account [4, 5]. The four-sample coning correction of *Algorithm 7* in [29], and the four-sample sculling correction of *Algorithm 5* in [30] are employed. As for the functional iteration algorithm, the maximum degrees of Chebyshev polynomials used to fit the angular velocity, specific force and gravity vector as well as the truncation degrees of attitude, velocity, and position are set to be the same as [14]. The convergence criterion of iteration is set to 10^{-16} , and the maximum number of attitude iteration and velocity/position iteration are set as $N+1$, where N denotes the number of samples.

Fig. 1 presents the principal attitude error, velocity and position errors of different algorithms for the coning frequency $f_c = 0.037 \text{ Hz}$. Note that the compensation for the rotation effect of navigation frame has been taken into account for all the traditional/enhanced algorithms, and the velocity/position integration formula with navigation reference frame rotation considered (named the VPifNav algorithm [21]) is also compared to highlight the significance of navigation reference frame rotation effect. It is observed that the enhanced algorithms achieve a similar level of accuracy as the traditional algorithms, for both the two-sample and four-sample cases. It echoes with the above analytical analysis that the accuracy improvement of the enhanced algorithms is indeed marginal as compared to the corresponding traditional algorithms. Furthermore, the functional iteration algorithms have significant accuracy superiority over all the traditional/enhanced algorithms, no matter for the two-sample or four-sample case. In addition, it is worth noting that the work [13] just provides a coarse navigation- rotation compensation, while our previous paper [21] provides a more rigorous and precise rotation compensation and exhibits superior accuracy to the traditional/enhanced algorithms, as shown in Fig. 1.

In order to assess the algorithms under a range of different dynamic conditions, the coning frequencies are set to vary within 0.01-20 Hz. Fig. 2 plots the principal attitude error, magnitudes of velocity error and position errors as the function of relative frequency f_c / f_s , and Table III lists the specific maximum west-east position errors at three representative coning frequencies for demonstration.

Table III
Summary of Maximum West-East Position Errors at Representative Coning Frequencies.

	$f_c = 0.037 \text{ Hz}$	$f_c = 0.185 \text{ Hz}$	$f_c = 1 \text{ Hz}$
Typical (N=2)	16.83 m	16.95 m	965.18 m
Enhanced (N=2)	16.83 m	16.80 m	980.98 m
VPifNav (N=2)	3.17 m	2.93 m	970.28 m
iNavFIter (N=2)	$7.34 \times 10^{-5} \text{ m}$	0.20 m	929.31 m
Typical (N=4)	33.72 m	34.85 m	137.88 m
Enhanced (N=4)	33.71 m	34.11 m	24.63 m
iNavFIter (N=4)	$3.37 \times 10^{-6} \text{ m}$	$1.35 \times 10^{-5} \text{ m}$	2.40 m
iNavFIter (N=8)	$4.27 \times 10^{-6} \text{ m}$	$4.36 \times 10^{-6} \text{ m}$	$2.05 \times 10^{-5} \text{ m}$

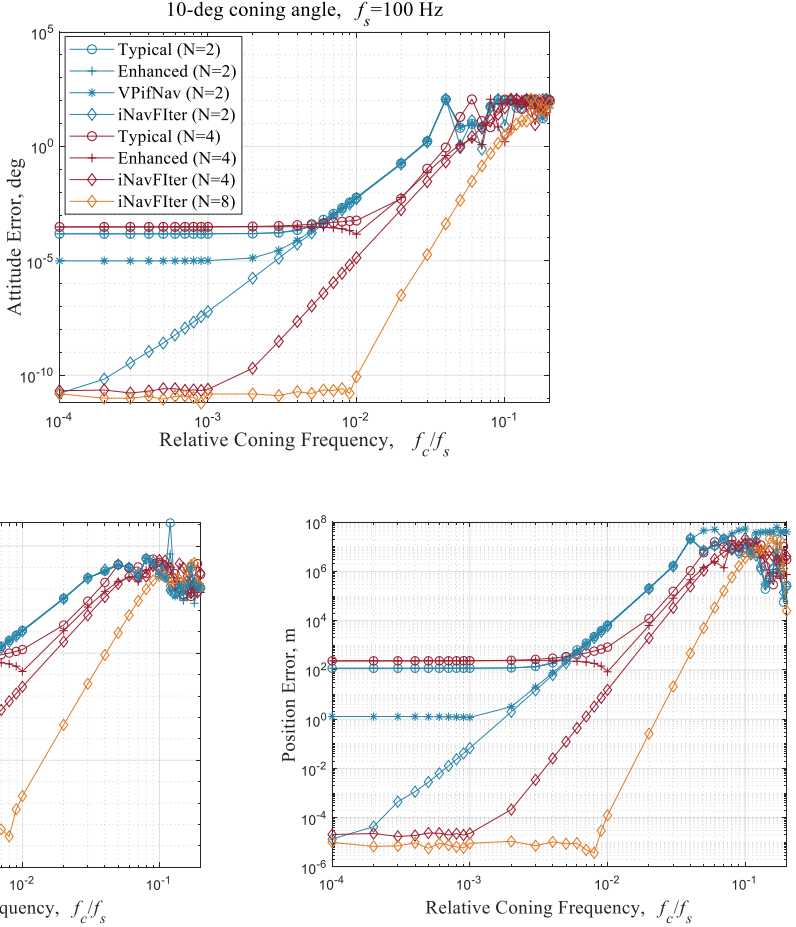


Fig. 2. Principal attitude error, magnitudes of velocity error and position error as a function of relative frequency.

It can be seen that the enhanced algorithm achieves nearly identical accuracy to the traditional algorithm for the two-sample case. As for the four-sample case, when the relative frequency is below 0.006, the enhanced algorithm achieves the same level of accuracy as the traditional algorithm, but when the relative frequency surpasses this threshold, the enhanced algorithm demonstrates a marginal improvement over the traditional one. In addition, at low relative frequencies, the functional iteration two-sample algorithm exhibits a substantial accuracy superiority over both the traditional/enhanced two-sample and four-sample algorithms. This superiority becomes more pronounced with an increasing number of samples, as evidenced by the iNavFIter (N=4) and iNavFIter (N=8) in Fig. 2. However, at high coning frequencies, the accuracies of the functional iteration two-sample algorithm and the traditional/enhanced two-sample algorithms are comparable, so is the corresponding four-sample algorithms. The underlying reason is that

whether two samples or four samples are used to fit the measurements of gyroscopes and accelerometers, they would encounter significant angular velocity/specific force fitting errors at high coning frequencies, which dominates the inertial navigation computation errors in any algorithm (including the functional iteration). Therefore, for a high coning frequency, more samples are preferred to reduce the fitting errors as much as possible, as shown by the orange diamond-decorated curves in Fig. 2 for iNavFIter (N=8). Nevertheless, the number of samples cannot be increased without limit, as the interpolation quality on the equispaced sampling points is affected by the Runge phenomenon [31].

Furthermore, it may be surprising at first glance that the traditional/enhanced algorithms have relatively high errors in lowly dynamic conditions. The rationale is, on one hand, the approximate error in the traditional velocity update equation has remarkably negative impact on the attitude computation; on the other hand, the determination of the rotation vector in the navigation

frame introduces significant approximation errors, further amplifying the negative impact on the overall attitude computation. Moreover, the insufficient compensation of the navigation reference frame rotation issue also results in considerable error, as evidenced by the curves of the VPifNav algorithm. However, along with the increase of coning frequency, the dynamics of the body frame is strengthened and the error caused by the above factors is no longer dominant, which explains the curve coincidence of the traditional/enhanced two-sample algorithms and the VPifNav algorithm at high coning frequencies. Surprisingly, the two-sample algorithms slightly outperform the four-sample algorithms at lower frequencies. We speculate that this phenomenon is caused by a halved update frequency compared to the two-sample case that affects the navigation frame-related attitude/velocity computation.

In summary, no matter for a low or high coning frequency, the enhanced algorithms show marginal accuracy improvement over the traditional algorithms under the test scenarios in this paper, for both the two-sample and four-sample cases. Notably, the functional iteration approach possesses significant accuracy superiority even in sustained lowly dynamic conditions.

V. CONCLUSION

This paper investigates and compares the accuracy performance of the traditional/enhanced algorithms against the functional iteration algorithm. With the help of MATLAB Symbolic Toolbox, the analyses show that the error order of the traditional attitude algorithm is noticeably reduced by the enhanced algorithm, but the traditional velocity algorithm error order has not been effectively reduced by the corresponding enhanced algorithm. Numerical results in both the two-sample and four-sample cases indicate that the enhanced algorithms bring marginal improvement relative to the traditional algorithms, especially for the two-sample algorithms. This phenomenon is arguably caused by the coupling effect among the attitude, velocity, and position computation. Meanwhile, the functional iteration algorithm still has a significant accuracy superiority in sustained lowly dynamic conditions including large-amplitude, low-frequency motions. For the highly dynamic motion, it is necessary to appropriately increase the number of samples to improve the computation accuracy of any algorithm, as reported in the previous literature.

VI. ACKNOWLEDGMENT

The authors sincerely thank the reviewers, the associate editor, and Dr. Yury A. Litmanovich for their constructive comments and suggestions, which greatly improved the quality of the paper.

Hongyan Jiang

Maoran Zhu

Yuanxin Wu

Shanghai Jiao Tong University, Shanghai, China

REFERENCES

- [1] P. D. Groves, *Principles of GNSS, Inertial, and Multisensor Integrated Navigation Systems*, 2nd ed. Boston, MA, USA and London, U. K.: Artech House, 2013. Chap. 2.
- [2] M. B. Ignagni, *Strapdown Navigation Systems: Theory and Application*, Minneapolis, MN: Champlain Press, 2018. Chap. 5 and Chap. 6.
- [3] P. G. Savage, "Computational elements for strapdown systems," in *Low Cost Navigation Sensors and Integration Technology*, NATO Lecture Series RTÖ-EN-SET-116, 2008.
- [4] M. B. Ignagni, "Accuracy limits on strapdown velocity and position computations," *J. Guid., Control Dyn.*, vol. 44, no. 3, pp. 654-658, 2021.
- [5] M. B. Ignagni, "Enhanced strapdown attitude computation," *J. Guid., Control Dyn.*, vol. 43, no. 6, pp. 1220-1224, 2020.
- [6] L. Goodman and A. Robinson, "Effect of finite rotations on gyroscopic sensing devices," *J. Appl. Mech.*, vol. 25, pp. 210-213, June 1958.
- [7] P. G. Savage, "A new second-order solution for strapped-down attitude computation," *Guidance and Control Conference*, 1966.
- [8] J. W. Jordan, "An accurate strapdown direction cosine algorithm," *NASA, TN-D-5384*, Sept. 1969.
- [9] J. H. Laning, "The vector analysis of finite rotations and angles," Massachusetts, Ed., ed. Cambridge, MA: Massachusetts Inst. of Technology, Instrumentation Lab. Rept. 6398-S-3, 1949.
- [10] J. Bortz, "A new mathematical formulation for strapdown inertial navigation," *IEEE Trans. Aerosp. Electron. Syst.*, vol. 7, no. 1, pp. 61-66, 1971.
- [11] P. G. Savage, "A unified architecture for strapdown integration algorithms," *J. Guid., Control Dyn.*, vol. 29, no. 2, pp. 237-249, 2006.
- [12] R. B. Miller, "A new strapdown attitude algorithm," *J. Guid., Control Dyn.*, vol. 6, no. 4, pp. 287-291, 1983.
- [13] P. G. Savage, "Strapdown inertial navigation integration algorithm design Part 2: velocity and position algorithms," *J. Guid., Control Dyn.*, vol. 21, no. 2, pp. 208-221, 1998.
- [14] Y. Wu, "iNavFlter: next-generation inertial navigation computation based on functional iteration," *IEEE Trans. Aerosp. Electron. Syst.*, vol. 56, no. 3, pp. 2061-2082, 2020.
- [15] M. B. Ignagni, "On the orientation vector differential equation in strapdown inertial systems," *IEEE Trans. Aerosp. Electron. Syst.*, vol. 30, no. 4, pp. 1076-1081, 1994.

[16] H. Musoff and J. H. Murphy, "Study of strapdown navigation attitude algorithms," *J. Guid., Control Dyn.*, vol. 18, no. 2, pp. 287-290, 1995.

[17] V. Z. Gusinsky, V. M. Lesyuchevsky, Y. A. Litmanovich, H. Musoff, and G. T. Schmidt, "New procedure for deriving optimized strapdown attitude algorithms," *J. Guid., Control Dyn.*, vol. 20, no. 4, pp. 673-680, 1997.

[18] G. M. Yan, W. S. Yan, and D. M. Xu, "Limitations of error estimation for classic coning compensation algorithm," *9th International Conference on Electronic Measurement & Instruments*, 2009.

[19] M. Song, W. Wu, and J. Wang, "Error analysis of classical strapdown velocity integration algorithms under maneuvers," *J. Guid., Control Dyn.*, vol. 36, no. 1, pp. 332-337, 2013.

[20] Y. Wu and X. Pan, "Velocity/position integration formula Part I: application to in-flight coarse alignment," *IEEE Trans. Aerosp. Electron. Syst.*, vol. 49, no. 2, pp. 1006-1023, 2013.

[21] Y. Wu and X. Pan, "Velocity/position integration formula Part II: application to strapdown inertial navigation computation," *IEEE Trans. Aerosp. Electron. Syst.*, vol. 49, no. 2, pp. 1024-1034, 2013.

[22] Y. Wu, "RodFlter: attitude reconstruction from inertial measurement by functional iteration," *IEEE Trans. Aerosp. Electron. Syst.*, vol. 54, no. 5, pp. 2131-2142, 2018.

[23] Y. Wu, Q. Cai, and T.-K. Truong, "Fast RodFlter for attitude reconstruction from inertial measurements," *IEEE Trans. Aerosp. Electron. Syst.*, vol. 55, no. 1, pp. 419-428, 2019.

[24] Y. Wu and G. Yan, "Attitude reconstruction from inertial measurements: QuatFlter and its comparison with RodFlter," *IEEE Trans. Aerosp. Electron. Syst.*, vol. 55, no. 6, pp. 3629-3639, 2019.

[25] Y. Wu and Y. A. Litmanovich, "Strapdown attitude computation: functional iterative integration versus Taylor series expansion," *Gyroscopy Navig.*, vol. 11, no. 4, pp. 263-276, 2021.

[26] D. H. Titterton and J. L. Weston, *Strapdown Inertial Navigation Technology*, 2nd ed. Institute of Electrical Engineers, London, 2004. Chap. 11.

[27] M. B. Ignagni, "Optimal strapdown attitude integration algorithms," *J. Guid., Control Dyn.*, vol. 13, no. 2, pp. 363-369, 1990.

[28] P. G. Savage, "Strapdown inertial navigation integration algorithm design Part 1: attitude algorithms," *J. Guid., Control Dyn.*, vol. 21, no. 1, pp. 19-28, 1998.

[29] M. B. Ignagni, "Efficient class of optimized coning compensation algorithms," *J. Guid., Control Dyn.*, vol. 19, no. 2, pp. 424-429, 1996.

[30] M. B. Ignagni, "Duality of optimal strapdown sculling and coning compensation algorithms," *Navigation*, vol. 45, no. 2, pp. 85-95, 1998.

[31] Y. Wu and M. Zhu, "Attitude reconstruction from inertial measurement mitigating Runge effect for dynamic applications," *IEEE Trans. Aerosp. Electron. Syst.*, vol. 58, no. 2, pp. 1257-1265, 2022.